Photodynamical Effects Induced by the Angular Momentum of Light in Liquid Crystals

G. Abbate, P. Maddalena, L. Marrucci, L. Saetta and E. Santamato

Dipartimento di Scienze Fisiche, Pad.20 Mostra d'Oltremare, 80125 Napoli, Italy

Abstract

We report the observation of a very rich reorientational dynamics of the molecular director of a 5CB nematic film, induced by an elliptically polarized c.w.-laser beam above the threshold for the Optical Frèedericksz Transition. In despite of the very complicated character of the observed motions, a simple model, based on continuum theory and angular momentum conservation reproduces very well the experimental findings.

1. Introduction

Laser-beam propagation in nematic liquid crystals exhibits very unique and fascinating nonlinear optical effects. It has been demonstrated that a cw laser beam focused to an intensity of the order of $1\,\mathrm{kW\,cm^{-2}}$ can induce a Frèedericksz transition (an orientational transition) in a nematic film [1]. It was also shown that a *time-dependent* polarization rotation is induced in a homeotropically aligned liquid-crystal film by a circularly polarized c.w.-laser beam at normal incidence [2]. This remarkable effect was later ascribed to a new nonlinear optical effect, Self-Induced Stimulated Light Scattering [3]. The phenomenon is caused by the constant deposition of angular momentum from the field to the medium, inducing a collective uniform precession of the liquid crystal molecules about the beam propogation direction. In the process, energy is dissipated by viscous forces in the liquid crystal. Since the medium is transparent, the energy loss appears as a red shift on part of the beam. This red shift was also measured [4].

Self-Induced Stimulated Light Scattering occurs also when an *elliptically* polarized laser beam is sent onto a homeotropically aligned liquid-crystal film, but, in this case, the process becomes much more complicated, because both circular components σ^+ and σ^- are present in the incident beam. Photons σ^+ and σ^- transfer opposite angular momenta to the medium so that the actual torque on the molecules of the liquid crystal depends on their delicate balancing. Moreover, the azimuthal symmetry of the system (field and matter) is broken. Thus, the elliptically polarized input can lead the system through various dynamic regimes: torsional oscillation, nonuniform precession, nutation superimposed on precession and others. Experimental observations are in good agreement with theoretical prediction from a continuum model of laser-beam propagation in an anisotropic fluid with reorientational internal degrees of freedom [5].

The case of linear polarization at normal incidence is exceptional in the sense that no angular momentum is transferred to the medium along the beam direction. This results in a simpler dynamics in which the system always reaches a final equilibrium state [1]. Nevertheless, both theory and experiment demonstrate that also in this case angular momentum transfer from the optical field to the medium plays an important role, producing the occurrence of remarkable nonlinear optical phenomena like multistability, hysteresis and optical phase locking [6].

It is worth noting that all these effects are not observed when a liquid crystal film is reoriented by a *static* (electric or magnetic) field. This is to be ascribed ultimately to the fact that optical fields, unlike static fields, do carry angular momentum.

In this work we present a brief review of our experimental observations about the photodynamical effects induced in a nematic liquid crystal film by an elliptically polarized c.w.-laser beam. We present also a unified physical interpretation of these phenomena in terms of direct exchange of angular momentum between the radiation and the liquid crystalline medium.

2. The role of the angular momentum of light

Unlike ordinary liquids, liquid crystals have extra internal degrees of freedom, describing the collective local orientation of the molecules. In the mesophases, molecular fluctuations can be neglected and their local orientation can be described by a unit vector $n(r, t)$, yielding the average direction of the molecules in a small volume element located at r at time t. For nematics, the equilibrium distribution of $n(r, t)$ is obtained by minimizing the Franck–Oseen elastic distortion free energy $E_d = \int F_d \, dV$, whose density F_d is given by

$$F_d = \tfrac{1}{2}[K_{11}(\operatorname{div} n)^2 + k_{22}(n \cdot \operatorname{rot} n)^2 + k_{33}(n \times \operatorname{rot} n)^2] \quad (1)$$

under the constraints imposed by boundary conditions at the sample walls.

Consider a monochromatic optical field of frequency ω propagating in the nematic liquid crystal. The total free energy density F is then obtained by adding to eq. (1) the average energy density W of the electromagnetic field:

$$W = (1/16\pi)(D \cdot E^* + B \cdot H^*). \quad (2)$$

We assume the medium non absorbing, nonmagnetic ($B = H$), and uniaxial with the optical axis along n:

$$D_i = \varepsilon_{ij}E_j = \varepsilon_\perp E_i + \varepsilon_a n_i n_j E_j$$

$$(i, j = 1, 2, 3; \text{ summation on } j), \quad (3)$$

where $\varepsilon_a = \varepsilon_\| - \varepsilon_\perp$ is the dielectric anisotropy. Since we are interested in varying the total free-energy with respect to the electric field E, we need the thermodynamic potential $\tilde{F}$ given by

$$\tilde{F} = F - (1/8\pi)(D \cdot E^*)$$

$$= F_d - (1/16\pi)(D \cdot E^* - H \cdot H^*). \quad (4)$$

For monochromatic optical field we have

$$H = -(1/k_0)\,\text{rot}\,E; \qquad k_0 = \omega/c. \qquad (5)$$

Inserting eq. (5) into eq. (4) we obtain $\tilde{F}$ as a function of n, E, E^*, and their spatial derivatives. We can then consider $\tilde{F}$ as a Lagrangian density to obtain the steady-state fields E, E^* and n from the variational principle

$$\delta \int (\tilde{F} + \mu n^2)\,dV = 0, \qquad (6)$$

where $\mu(r)$ is a suitable Lagrange multiplier accounting for the constraint $n^2 = n \cdot n = 1$. It easily found that the field equations associated to the variational principle (6) are Maxwell's equations for a monochromatic field:

$$\text{rotrot}\,E = k_0{}^2 D \qquad (7)$$

and the torque equations for the director n:

$$n \times h + t = 0, \qquad (8)$$

where h is the elastic part of the "molecular field" [7], having components

$$h_i = \partial_j[\partial F_d/\partial(\partial_j n_i)] - \partial F_d/\partial n_i, \qquad (9)$$

and

$$t = (1/8\pi)\,\text{Re}\,[D \times E^*] \qquad (10)$$

is the torque per unit volume due to the optical field.

Equations (8) hold in stationary case only. When n depends on time explicitly appropriate viscous terms must be added [8].

The advantage of using the variational principle (6) is that we can easily obtain conserved quantities by exploiting the invariance properties of the Langrangian density. The invariance of $\tilde{F}$ with respect to the gauge change $E \rightarrow Ee^{i\delta}$ (δ real and constant) leads to the conservation of the electromagnetic energy flux

$$\text{div}\,S = 0; \qquad S = (c/8\pi)\,\text{Re}\,(E \times H^*)$$

$$= \text{Poynting vector.} \qquad (11)$$

The invariance of $\tilde{F}$ with respect to translations of the coordinate frame leads to the conservation of the flux of the total (fluid + optical field) linear momentum

$$\partial_i \sigma_{ij} = \partial_i[(\sigma_d)_{ij} + \hat{T}_{ij}] = 0, \qquad (12)$$

where in the total stress tensor σ_{ij} we have split the part $(\sigma_d)_{ij}$ due to the reorientational distortion and the part $\hat{T}_{ij}$ due to the presence of the optical field:

$$\hat{T}_{ij} = (H_{ik}\partial_j E_k{}^* + \text{c.c.}) - \delta_{ij}(1/16\pi)(D \cdot E^* - H \cdot H^*), \qquad (13)$$

where

$$H_{ik} = (1/16\pi k_0{}^2)(\partial_i E_k - \partial_k E_i). \qquad (14)$$

Relation (12) states that, at equilibrium, the elastic forces balance the electrostrictive forces due to the optical field.

Finally, the invariance with respect to rotations of the coordinate frame leads to the conservation of the flux of total angular momentum

$$\partial_i M_{ijk} = \partial_i[(M_d)_{ijk} + \overset{\circ}{M}_{ijk}] = 0, \qquad (15)$$

where $(M_d)_{ijk}$ and $\overset{\circ}{M}_{ijk}$ are the contributions of the molecular distortion and of the optical field, respectively, given by

$$[\pi_{ij} = \partial\tilde{F}/\partial(\partial_i n_j)]$$

$$(M_d)_{ijk} = [(\sigma_d)_{ij}x_k - (\sigma_d)_{ik}x_j] + (\pi_{ij}n_k - (\pi_{ij}n_k - \pi_{ik}n_j)$$

$$\overset{\circ}{M}_{ijk} = [\hat{T}_{ij}x_k - \hat{T}_{ij}x_j] + (H_{ij}E_k{}^* - H_{ik}E_j{}^* + \text{c.c.}). \qquad (16)$$

The tensors M_d and $\overset{\circ}{M}$ are not symmetric [9], but they are naturally split in an *orbital part* (in square brackets) and in an *intrinsic* part. The intrinsic part does not depend on the position r explicitly.

One can verify that eqs. (15) are equivalent to the torque eqs.(8). Equations (8) express, therefore, that, at equilibrium, the torque acting on each volume of the medium is due the angular momentum deposited there by the optical field, as we anticipated in the Introduction.

The conservation laws (11), (12), and (15) can be rewritten as surface integrals on the sample walls:

$$\oint_{\partial V} (u \cdot S)\,d\sigma = 0; \quad \oint_{\partial V} f\,d\sigma = 0; \quad \oint_{\partial V} \mu\,d\sigma = 0, \qquad (17)$$

where u is the normal to the surface element $d\sigma$ on ∂V and S, f, μ are the fluxes of energy, linear momentum, and angular momentum traversing $d\sigma$, respectively. In particular, the flux of angular momentum carried by the optical field is $\hat{\mu} = \hat{\mu}^{\text{orb}} + \hat{\mu}^{\text{int}}$, with

$$\hat{\mu}^{\text{orb}} = r \times \hat{f}$$

$$\hat{\mu}^{\text{int}} = (1/8\pi k_0)\,\text{Im}\,[E^* \times (u \times H)], \qquad (18)$$

where

$$\hat{f} = (1/8\pi k_0)\,\text{Im}\,[\Sigma_k(u \times H)_k\,\text{grad}\,E_k{}^*]$$

$$- u(1/16\pi)(D \cdot E^* - H \cdot H^*) \qquad (19)$$

is the linear momentum flux carried by the optical field.

It is interesting to see how the formulae above reduce in the important case of plane-wave. Let k be the wavevector and $\tilde{n} = k/k_0$ the corresponding unit vector. Let s be the unit vector along S, the energy flux. Then $s \cdot \tilde{n} = 1$. The group velocity v_g and the phase velocity v_f are defined by $v_g = cs$ and $v_f = (c/\tilde{n}^2)\tilde{n}$, respectively. $\tilde{n}$ is the refractive index as seen by the wave. In a birefringent medium, v_g and v_f are different. Then, a straightforward calculation shows that for a plane wave $S = cWs$, where $W = (1/8\pi)(\tilde{n}^2 E \cdot E^*)$ is the optical energy density and

$$\hat{f} = W(u \cdot s)\tilde{n}; \qquad \hat{\mu}^{\text{orb}} = r \times \hat{f}$$

$$\hat{\mu}^{\text{int}} = (1/8\pi k_0)\,\text{Im}\,[u(H \cdot E^*) - H(u \cdot E^*)]. \qquad (20)$$

It is worth noting that the first of eqs. (20) yields a picture where photons in a birefringent medium travel along the ray direction s, but carry a linear momentum along the phase direction $\tilde{n}$ (their quantum linear momentum is still $\hbar k$). We may also introduce the notion of average "spin" angular momentum flux ϕ along the direction of the linear momentum: only the intrinsic part will contribute and we obtain

$$\phi = (\tilde{n} \cdot \hat{\mu}^{\text{int}})/\tilde{n} = (1/8\pi k_0 \tilde{n})(\tilde{n} \cdot u)\,\text{Im}\,[H \cdot E^*]. \qquad (21)$$

For linear polarization of the wave, E and H are in phase and orthogonal each other. The average spin flux ϕ is then zero, but we may still have a nonzero contribution to the total angular momentum from the orbital part. In the case of elliptical polarization, eq.(21) can be rewritten as

$$\phi = (1/8\pi k_0 \tilde{n})(\tilde{n} \cdot u)\,\text{Im}\,[(E \times E^*) \cdot \tilde{n}]. \qquad (22)$$
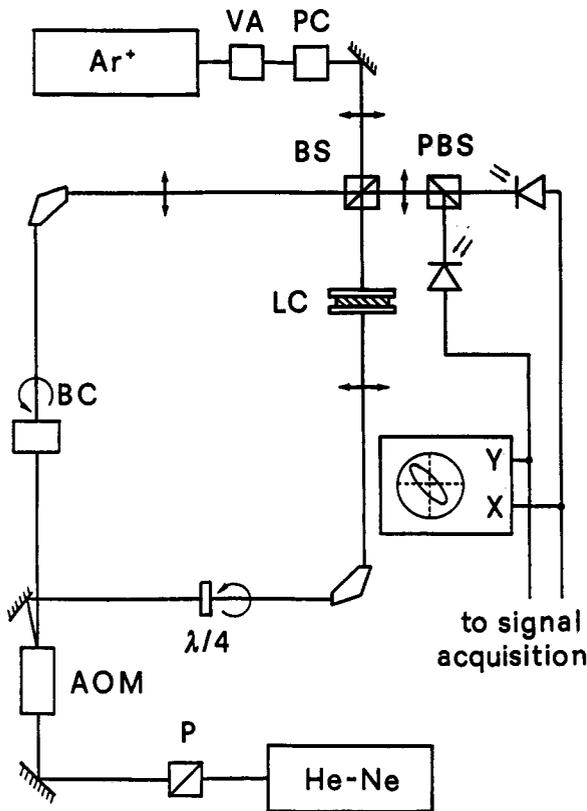
Fig. 1. Experimental set-up [AOM — Acousto-Optic Modulator; BC — Babinet Compensator; BS — Beam Splitter; LC — Liquid Crystal cell; P — Polarizer; PBS — Polarizing Beam Splitter; PC — Pockel's Cell; VA — Variable Attenuator].

Fig. 2. Zone diagram in the (χ, I) plane of the observed dynamical regimes: χ is the pump beam polarization ellipticity angle defined by $\sin 2\chi = s_3$ and $I/I_{th}(0)$ is the normalized beam intensity. Squares refer to steady-state regime, circles to oscillations, triangles to rotations; filled-in symbols refer to regimes observed by decreasing the intensity. Dashed line is the temperature corrected theoretical threshold intensity.

Choosing a local frame with the z-axis along the direction of k and taking u along z, we find

$$\phi/s_z = (1/\omega)\frac{2\text{Im}(E_x E_y)}{E \cdot E^*} \tag{23}$$

that reduces for isotropic media to the well-known Abraham-Sommerfeld formula for the photon spin [10].

3. The experiments

In our experiments we used a $75\,\mu m$-thick nematic film of 4-cyano-4'-pentyl-biphenyl (5CB) sandwiched between two glass plates coated with DMOAP for homeotropic alignment (molecular anchoring normal to the walls).

The experimental arrangement is shown in Fig. 1 The pump argon-laser beam ($\lambda = 0.515\,\mu m$) propagating along the z-axis was focused at normal incidence onto a 5CB sample by means of a 15-cm focal lens. The polarization and the intensity of the argon laser could be changed independently by a Pockel's cell and a variable attenuator. The optically-induced time-dependent molecular reorientation was probed through a counter-propagating He–Ne beam focused at the same point as the argon beam. The spots of the He–Ne and of the argon laser at the sample were $\simeq 70\,\mu m$ and $\simeq 120\,\mu m$ diameter, respectively. The probe He–Ne beam was circularly polarized by a $\lambda/4$ plate put in front of the sample and inserted in a heterodyne interferometer/polarimeter scheme [11]. The heterodyne polarimeter was already described in Ref. 2, to which we refer for details. This apparatus permits a real-time monitoring of the complete polarization state of the He–Ne beam after its passage through the sample. 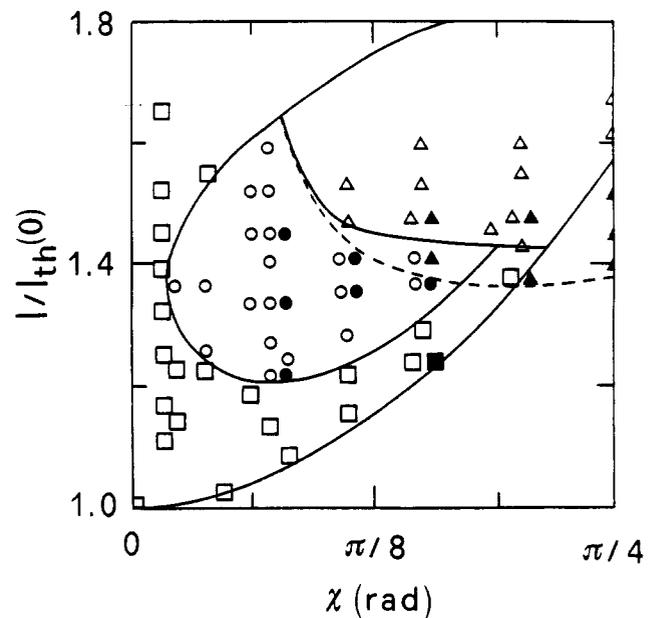The polarization ellipse of the He–Ne beam could be either observed directly on the screen of a digital oscilloscope or sent to a vectorial voltmeter and/or to an IBM-PC computer for data processing. Circular polarization was chosen for the probe beam in order to decouple the polar and azimuthal degrees of freedom of the molecular director during the observations.

The data were taken by fixing the polarization of the argon beam by the Pockels cell and varying its intensity in steps of about 5 mW each. After each intensity change, we waited until the final regime was attained. The transients ranged from about 30 to 60 s, a much longer time than the relaxation time at laser switching off, which was of a few seconds. When a given regime was reaached, however, it remained stable for hours.

In the case of elliptical polarization, different dynamical regimes were observed, depending on the polarization ellipticity s_3 and on the intensity I of the pump beam. Our observations are summarized in Fig. 2, where the plane (s_3, I) of the control parameters has been divided in several regions, pertaining to different kinds of motions induced in the sample. In the figure, the intensity I is normalized to the intensity $I_{th}(0)$ needed to induce the optical Fréedericksz transition for linear polarization of the argon beam. The ratio $I/I_{th}(0)$ was determined experimentally by the corresponding input power ratio, without any need of accurate determination of the beam cross-section at the sample, which usually introduces large errors in the measurements.

Let us describe the laser-induced reorientation in the liquid crystal sample by the polar angles (ϑ, ϕ) of the molecular director N. For a fixed ellipticity, no reorientation was observed in the sample until the intensity threshold I_{th} for the optical Fréedericks transition was reched. Let us consider the case of general elliptical pump polarization first. Slightly above the threshold, the azimuthal and the polar angles ϕ and ϑ of n were found to reach a final steady-state. At higher argon intensities, the molecular director undergoes a small
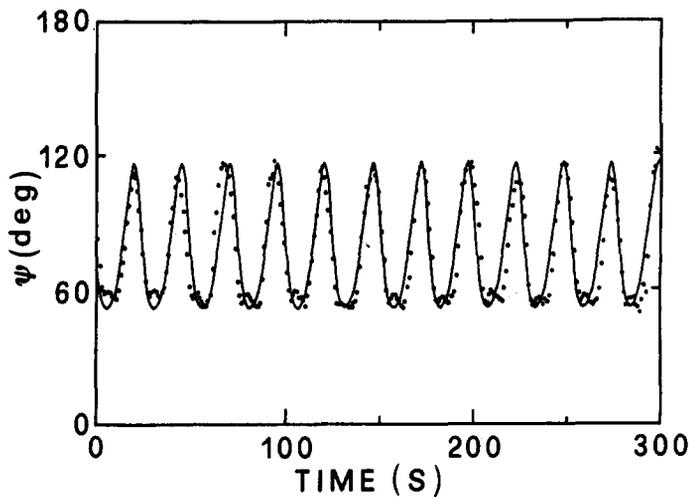
Fig. 3. Typical oscillatory regime observed for $\chi = 0.35$ rad and $I/I_{th}(0) = 1.53$ [ψ is the angle between the polarization ellipse major axis and a reference direction].

irregular fluctuation around its equilibrium position, that gets stronger and more regular increasing the pump power, until persistent neat oscillation of ϕ and ϑ occurs. The transition from the "noisy" steady-state and the persistent oscillations regime is smooth. An example of these oscillations is shown in Fig. 3. At higher intensities, a new critical value of I is attained, beyond which the director n starts to precess continuously around the beam propagation direction. The switching to precession is discontinue. The angular velocity of the precession motion is *not uniform*, in general, and it is always associated to nutation. The presence of nutation is manifested by the oscillation in time of the ellipticity s_3 of the probe beam emerging from the sample. The presence of precession is manifested by the rotation of the polarization ellipse of the probe beam, as shown in Fig. 4.

When the pump intensity is lowered, the persistent oscillation regime is reached again, but at a lower transition intensity. In other words, hysteresis was found between the two *time-dependent* stable states of persistent oscillations and of precession/nutation motion. This is shown by the dashed region in Fig. 2. As long as it concerns the transition back from the persistent oscillation regime to the steady-state regime, we observed regular oscillation at intensities where before irregular fluctuations were found. Unlike the case of
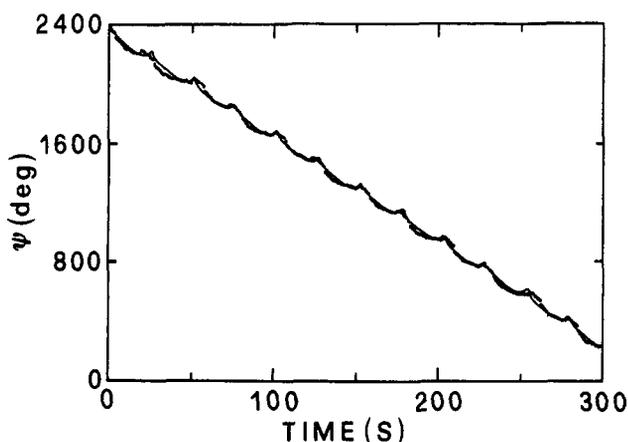

Fig. 4. Typical rotatory regime observed for $\chi = 0.35$ rad and $I/I_{th}(0) = 1.53$ [ψ is the angle between the polarization ellipse major axis and a reference direction].

increasing intensities, the transition to the steady-state regime is now sharp.

In the case of circular polarization, oscillations were absent and, above the threshold, the system was put directly into a uniform rotatory motion, as already reported in Ref. 1. The direct transition to rotation was observed also for ellipticity values close to the circular one. Finally, in the case of linear pump polarization, a monotonic decay towards a final steady-state was always observed, above the threshold. All these regimes are also shown in Fig. 2.

4. Discussion

We now consider some quantitative features of the observed phenomena. The threshold I_{th} for the Fréedericksz transition is given by [12]

$$I_{th} = \frac{2I_{th}(0)}{1 + \sqrt{1 - s_3^2}}, \tag{24}$$

where $I_{th}(0)$ is the threshold for linear polarization and s_3 is the ellipticity of the incident beam. Relation (24) shows that for circular polarization the threshold should be twice $I_{th}(0)$. From our measurements we found a ratio $I_{th}(1)/I_{th}(0) \cong 1.6$. The discrepancy with respect to the theoretical ratio of 2 is far beyond the experimental errors. We ascribe this to thermal effects due to laser heating. The material constants [which are encoded in $I(0)$] are temperature dependent, in fact, since the order parameter S of the nematic material changes with temperature according to the empiric law (for 5CB) [13]

$$S = (1 - T/T^*)^{0.22}. \tag{25}$$

Where T^* is an effective temperature very close to the nematic to isotropic transition temperature. T^* was experimentally related to the intensity I^* to which the clearing of the sample was observed. The resulting temperature corrected threshold curve as a function of ellipticity is drawn in Fig. 2. The agreement with experiment is good.

The equations of motion (8) governing the molecular director n and the evolution of the polarization of the incoming beam in traversing the medium have been numerically integrated by using a library routine for parabolic partial differential equations on a Digital VAX 2000 station. In the numerical computation, tabulated values were used for the material constants of 5CB [14] ($k_{11} = 0.7 \times 10^{-6}$ dyne, $k_{22} = 0.5 \times 10^{-6}$ dyne, $k_{33} = 0.9 \times 10^{76}$ dyne, $n_o = 1.52$, $n_e = 1.7$), without any fitting procedure. The results are in excellent agreement with the experimental observations, as shown by the full-line curves in Figs. 3 and 4. The model yields also the correct succession of the observed dynamical regimes for any fixed laser ellipticity, as reported in Fig. 2 (see Ref. [5]).

Acknowledgements

References

1. See. for example, Durbin S. D., Arakelian, S. M. and Shen, Y. R., Phys. Rev. Lett. 47, 1411 (1981).
2. Santamato, E., Daino, B., Romagnoli M., Settembre, M. and Shen, Y. R., Phys. Rev. Lett. 57, 2423 (1986).

3. Santamato, E., Romagnoli M., Settembre, M., Daino, B. and Shen, Y. R., Phys. Rev. Lett. **61**, 113 (1988).

4. Santamato, E., Daino, B., Romagnoli M., Settembre, M. and Shen, Y. R., Mol. Cryst. Liq. Cryst., **143**, 89 (1986).

5. Santamato, E., Abbate, G., Maddalena, P., Marrucci, L. and Shen, Y. R., Phys. Rev. Lett., **64**, 1377 (1990).

6. Abbate, G., Maddalena, P., Marrucci, L., Saetta, L. and Santamato, E., work presented at the III International Topical Meeting on "Optics of Liquid Crystals", Cetraro, Italy, 1-5 October (1990).

7. DeGennes, P., "The Physics of Liquid Crystals", Clarendon Press, Oxford, 1979, Chap. III.

8. The explicit expressions for the elastic, viscous, and optical torques as functions of the angles ϑ and ϕ of the director n and of the Stokes parameters of the incident beam in the plane-wave approximation can be found in Santamato, E., Abbate, G. and Maddalena, P., Phys. Rev. **A38**, 4323 (1988).

9. They can be symmetrized, of course, by adding a suitable term having the form $\partial_k f_{ijk}$ with $f_{ijk} = -f_{kij}$, but this would mix the orbital and intrinsic part of the initial tensors.

10. Unlike more standard approaches [Humblet, J., Physica, **10**, (1943)], the present one yields correct results also in the case of plane wave, without having recourse to boundary terms at infinite.

11. Buhrer, C. F., Bloom, L. R. and Baird, D. H., Appl. Opt, **2**, 839 (1963); Calvani, R., Caponi, R. and Cisternino, F., Opt. Comm. **54**, 63 (1985).

12. Zel'dovich, B. Ya. and Tabirian, N. V., Zh. Eksp. Teor. Fiz. **82**, 167 (1982). [Sov. Phys. JEPT **55**, 99 (1982). The same result is obtained also from eqs. (8).

13. Khoo, I. C., IEEE J. Quantum Electronics, vol. QE-**22**, no. 8, 1268 (1986).

14. Skarp, K., Lagerwall, S. T. and Stebler, B., Mol. Cryst. Liq. Cryst. **60**, 215 (1980).